Journal of Statistical Physics, Vol. 75, Nos. 5/6, 1994

Chaotic Cascades with Kolmogorov 1941 Scaling

L. Biferale,[1] **M. Blank,**[1,2] **and U. Frisch**[1]

Received November 9, 1993; final March 2, 1994

We define a (chaotic) deterministic variant of random multiplicative cascade models of turbulence. It preserves the hierarchical tree structure, thanks to the addition of infinitesimal noise. The zero-noise limit can be handled by Perron–Frobenius theory, just like the zero-diffusivity limit for the fast dynamo problem. Random multiplicative models do not possess Kolmogorov 1941 (K41) scaling because of a large-deviations effect. Our numerical studies indicate that *deterministic* multiplicative models can be chaotic and still have exact K41 scaling. A mechanism is suggested for avoiding large deviations, which is present in maps with a neutrally unstable fixed point.

KEY WORDS: Fully developed turbulence; chaotic maps; large deviations; transfer matrix; dynamo theory.

1. INTRODUCTION

One popular way to describe the small-scale activity of fully developed turbulence is to suppose that energy is transferred from the injection scale to the viscous scales by a multistep process along the inertial range. This idea has been often used to predict important features of turbulent flows. Still, relations with the structure of Navier–Stokes equations are poorly understood.

In his 1941 work, Kolmogorov[1] uses his phenomenology to postulate that all the statistical properties of the turbulent flow at scales belonging to the inertial range are *universal*, in the sense that they depend only on the scale l and on the mean energy dissipation rate per unit mass $\bar{\varepsilon}$. As a consequence, moments of velocity increments, over small distances l, should

[1] CNRS URA 1362, Observatoire de Nice, BP 229, 06304 Nice Cedex 4, France.
[2] Russian Academy of Sciences, Institute for Information Transmission Problems, 101447, Moscow, Russia.

0022-4715/94/0600-0781$07.00/0 © 1994 Plenum Publishing Corporation

possess universal forms. This led Kolmogorov to dimensionally-based expressions for the structure functions:

$$S_l^{(p)} \equiv E\{\delta v_l^p(x)\} \equiv E\{(v(x+l)-v(x))^p\} \sim (\bar{\varepsilon}l)^{p/3} \tag{1}$$

where $E\{\cdots\}$ denotes ensemble average and the symbol $\sim$ means equality within $O(1)$ multiplicative constants. Thus (1) predicts scaling behavior for the structure functions, the function of order p having the exponent $\zeta_p = p/3$.

Although early experimental data seemed to confirm the prediction (at least for $p=2$), the K41 theory has been criticized because it does not take into account the natural (and also experimentally verified) presence of fluctuations in the energy dissipation. These fluctuations are commonly believed to be the consequence of the chaotic transfer of excitations along the inertial range. A possible way to account for this effect, suggested by Obukhov,[2] is the following. First, one introduces the average rate of energy dissipation over a cubic box $\Lambda_l(x)$ of side l centered on x:

$$\varepsilon_l(x) = \frac{1}{l^3}\int_{\Lambda_l(x)} \varepsilon(x)\,dx \tag{2}$$

Second, fluctuations in the velocity increment are related to fluctuations in $\varepsilon_l(x)$ by a "bridging relation" suggested by Kolmogorov's[1] theory, namely

$$\delta v_l^p(x) \sim (\varepsilon_l(x))^{1/3} \tag{3}$$

This bridging relation is still widely used. It has received good experimental support.[3] Still, it leads to some conceptual difficulties which are unrelated to the material to be presented in this paper.[4] From (2) and (3), we find

$$S_l^{(p)} \sim E\{\varepsilon_l^{p/3}\}\; l^{p/3} \tag{4}$$

Considerable experimental[5-7] and theoretical work[8,9,3] has been devoted in recent years to measuring and predicting the dependence of the quantities $E\{\varepsilon_l^{p/3}\}$ on the scale l. It seems that a certain consensus has been reached. From the experimental side, there is clear evidence of a nontrivial l dependence (at least for high-order moments). Similarly, from a theoretical point of view, all models based on *random* multiplicative cascades (Section 2) introduce power-law corrections to K41 scaling. The fact that these simple models have deviations to K41 scaling has led perhaps to the misconception that any cascade model having nontrivial fluctuations is inconsistent with K41 scaling.

Actually, we shall show that the chaotic transfer of energy described by a deterministic multiplicative process can still be consistent with K41, or more precisely that possible deviations disappear in the "fully developed limit," i.e., for cascades with very many steps.

The paper is organized as follows. In Section 2 we connect the well-known case of random independent multiplicative cascade models and our (deterministic) case in two steps. First, we introduce a Markov random model and then, by means of a special limiting construction, we obtain the deterministic model. A particular class of deterministic multiplicative models is introduced in Section 3 and studied numerically in Section 4. Finally, in Section 5 we give a possible interpretation of the lack of corrections to K41 scaling observed in our model.

2. PURE-RANDOM AND NOISY-DETERMINISTIC MULTIPLICATIVE MODELS

Random multiplicative models were introduced by Novikov and Stewart[13] and Yaglom[14] as a simple way to describe stochastic transfer of energy along the inertial range. Their fractal properties were discussed by Mandelbrot.[15] Let us give now the definition of these models. A binary tree structure, obtained by hierarchically partitioning the original volume of size l_0 into subvolumes of size $l_n = 2^{-n} l_0$, is used to describe fluctuations at different scales (Fig. 1a illustrates the one-dimensional case). The energy dissipation ε_n associated with a cube at scale l_n is multiplicatively linked to the energy dissipation ε_{n-1} at the larger scale l_{n-1} through a random variable W_n:

$$\varepsilon_n = W_n \varepsilon_{n-1} = W_n W_{n-1} W_{n-2} \cdots W_1 \bar{\varepsilon} \tag{5}$$

The W_n are identically and independently distributed positive random variables. The structure functions are now defined as

$$S_n^{(p)} \equiv E\{\varepsilon_n^{p/3}\}\, l_n^{p/3} \tag{6}$$

Using (4) and (5), we obtain

$$S_n^{(p)} = l_n^{\zeta(p)} \qquad \text{with} \quad \zeta(p) = p/3 - \log_2 E\{W^{p/3}\} \tag{7}$$

where $E\{\cdots\}$ denotes the mathematical expectation. Here, $-\log_2 E\{W^{p/3}\}$ is the correction to the K41 exponent in the structure function of order p. Actually, the multiplicative model (5) has very interesting properties when considered in the light of the theory of large deviations, as noted, in particular by Oono[16] and Collet and Koukiou.[17] It follows from Cramér's[18] work (see also refs. 19 and 20) that, for large n, the quantity

$$\frac{1}{n}\log_2 \varepsilon_n = \frac{1}{n}(\log_2 W_1 + \log_2 W_2 + \cdots + \log_2 W_n) \tag{8}$$

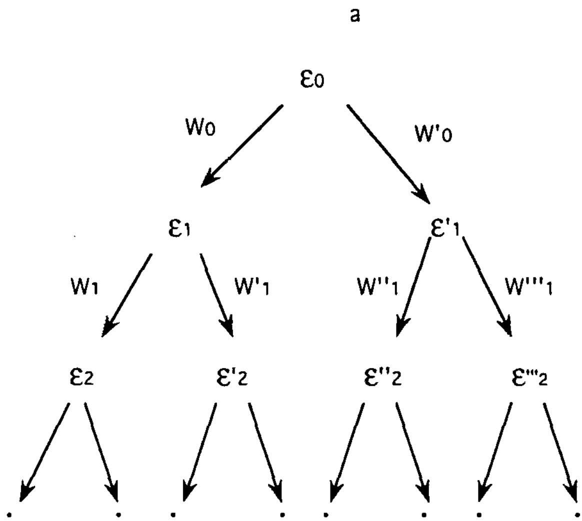

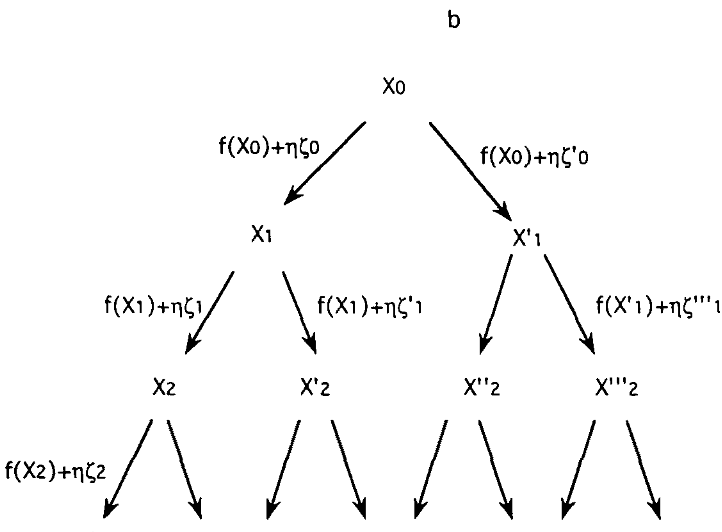

Fig. 1. (a) A one-dimensional representation of the dyadic tree for the random multiplicative chaos model. Each variable $\{W_i\}$ is chosen independently and identically distributed. (b) The branching process for the noisy deterministic maps; the ξ's are chosen independently on each link.

can deviate from its limit value $E\{\log_2 W\}$ by a finite, nonvanishing amount α with a probability which decreases as $\exp[-f(\alpha)n]$. The Cramér function[3] $f(\alpha)$ is positive and convex and can be identified with an entropy in applications to statistical thermodynamics.(20) The presence of such large deviations, with probability decreasing exponentially in n (i.e., as a power law in l_n), introduces fluctuations in the effective scaling exponent and therefore an overall change of the scaling properties of all structure functions. Indeed, we can rewrite (7) in the following form:

$$S_n^{(p)} \propto E\{\varepsilon_n^{p/3}\}\, l_n^{p/3} = E\{l_n^{-(p/3)(1/n)(\log_2 W_1 + \log_2 W_2 + \cdots + \log_2 W_n)}\}\, l_n^{p/3} \propto l_n^{\zeta_p} \quad (9)$$

As is well known, in large-deviations theory, the function $\zeta(p)$ is given by a Legendre transformation:

$$\zeta(p) = \inf_\alpha \left(\frac{p}{3}(1-\alpha) + \frac{f(\alpha)}{\ln 2}\right) \quad (10)$$

Our aim now is to construct a deterministic variant of such models. We shall do it in two steps. First, we consider, instead of independent random variables $\{W_i\}$, successive points on the orbit of a Markov process. This means that we consider a Markov process on a phase space X with a transition probability operator P and an observable $h: X \to R^1_+$. The (generalized) structure function at the scale $l_n = 2^{-n} l_0$ is then defined as

$$S_n^{(p)} = S_n^{(p)}[h, P] = E\left\{\prod_{k=1}^{n} h^p(x_k)\right\} \quad (11)$$

where $x_k \in X$ are points of an orbit of the Markov process. Introducing now

$$Z_n^{(p)} = \prod_{k=1}^{n} h^p(x_k) \quad (12)$$

we easily find that the conditional expectation of $Z_n(p)$ with respect to the initial distribution density $\rho(x)$ is given by

$$E\{Z_n^{(p)} \mid \rho\} = \int_X h^p(x)\, \rho(x)\, P_{h,p}^n 1(x)\, dx \quad (13)$$

Here, the operator $P_{h,p}$ is defined by the relation $P_{h,p}\phi(x) = h^p(x)\, P\phi(x)$. This concludes the first step. The second step is to change from a Markov *random* dependence to a *deterministic* dependence by use of a chaotic map.

[3] A name suggested by Mandelbrot.(21)

It seems that this can be done in an obvious way, replacing the transition probability operator by the transfer matrix (Perron–Frobenius operator) of the chaotic map. However, some additional work is needed to define a deterministic construction possessing the same tree structure as in the random case (Fig. 1a). Indeed, with a deterministic map, how can we avoid giving the same value to the two offsprings of the next generation, thereby trivializing the whole tree structure?

It is necessary to define a consistent procedure to distinguish the branches of the tree. We build up this branching-deterministic process by inserting a small amount of noise at each node and by considering the total process as the superposition of the deterministic transfer along consecutive levels plus the noise. The final map will be obtained by taking the zero-noise limit.

Let $f: X \to X \subset R^d$ be the deterministic map which describes the relation between any two consecutive scales of the tree structure (see Fig. 1b), and let us fix an observable $h: X \to R^1_+$. Then for any fixed number $\eta > 0$ we may consider a random Markov chain $(x_k^{(\eta)})$ such that

$$x_{k+1}^{(\eta)} = f(x_k^{(\eta)}) + \eta \xi_k \tag{14}$$

where the ξ_k are random variables, independently and identically distributed on the interval $[-1, 1]$. Now, we may apply the previous construction by considering different realizations of the noise ξ_k on each link connecting consecutive nodes. Then any cascade process along a branch of the tree in Fig. 1b will be described by the map (14) with different realizations of the noise.

We define our structure functions as the zero-noise limit of (11). For a fixed value of $\eta > 0$ it follows from (13) that the large-n limit of the structure functions is governed by the spectrum of the operator:

$$P_{h,p,\eta} = h^p Q_\eta P \tag{15}$$

Here, Q_η is the transition operator for the random perturbation, P is the transfer matrix, or Perron–Frobenius operator of the map f, and h is an observable (for definitions see, for example, ref. 22).

Let us mention, incidentally, that there is also another possibility to define a deterministic (chaotic) process on a tree structure. Using a method of finite-state Markov approximations of chaotic maps proposed by Ulam, we obtain a Markov chain with transition probabilities given by $p_{ij} = |X_i \cap f^{-1} X_j| / |X_i|$, where the set of X_i defines a suitable finite partition of the original phase space X. It is known, for instance, that for sufficiently "good" maps (for example, piecewise expanding with derivatives larger than two), invariant distributions of this simple Markov chain converge to the density of the invariant measure of the map under consideration when $|X_i| \to 0$. With this Markov process, we construct the analog of (15), namely the operator $P_{h,p} = h^p P$. (Here P is the transition operator with matrix elements p_{ij}.) These possibilities will not be explored further here.

We now observe that the construction based on taking the zero-noise limit appearing in (15) is similar to that of the mathematical theory of *fast dynamos.*[23-25] Fast dynamo theory describes the phenomenon by which rapid magnetic field growth can be sustained in the presence of a prescribed velocity field when taking the zero-diffusivity limit. From a formal point of view, fast dynamo theory involves a combination of two operators: a transfer matrix for some deterministic map, associated to a deterministic velocity field, and a diffusionlike operator, or equivalently small-amplitude noise.

The main purpose of the theory is then to find the properties of the zero-noise limit of the combined operator. Oseledets,[25] in his study of the dynamo problem, considered a noise-perturbed Perron–Frobenius operator similar to that of (15) and was able to show in special cases that it converges for $\eta \to 0$ to the Perron–Frobenius operator for the deterministic problem. The latter is than said to be "stochastically stable."

Returning to the structure function of the multiplicative model, we shall also assume that the Perron–Frobenius operator is stochastically stable. In addition, we assume that the map (14), with $\eta = 0$, is chaotic and ergodic. We can then compute the structure functions as averages along the orbit for the deterministic map, i.e.,

$$S_n^p = \lim_{N \to \infty} \frac{1}{N} \sum_{i=1}^{N} \prod_{k=1}^{n} h^p(x_{i+k}) \tag{16}$$

with $x_{i+1} = f(x_i)$.

3. A CLASS OF DETERMINISTIC CASCADE MODELS BASED ON SHELL MODELS

The construction defined in Section 2, after taking the zero-noise limit as explained, amounts simply to the following: we keep (5) as it stands, but instead of searching the W_n randomly, we assume that

$$W_n = g(W_{n-1}, W_{n-2}, \ldots, W_{n-r}) \tag{17}$$

where g is a deterministic map which involves a finite number r of antecedents. Although it is known that maps with only one antecedent can be chaotic, with the constraints that we shall use later, we shall need more than one antecedent.

There is an alternative formulation in terms of characteristic velocities associated with the hierarchy of scales $l_n = l_0 2^{-n}$. By analogy with (3), we introduce a set of velocity variables, denoted u_n, related to the ε_n by

$$\varepsilon_n = \frac{|u_n|^3}{l_n} \tag{18}$$

The u_n can be thought of as (real or complex) velocity amplitudes associated with eddy motion on scale l_n. Instead of (5) we then use

$$u_n = q_n q_{n-1} q_{n-2} \cdots q_1 u_0 \tag{19}$$

while (17) becomes

$$q_n = f(q_{n-1}, \dots, q_{n-r}) \tag{20}$$

Equation (20) will be called the "ratio map" since the q_n are the ratios of successive velocity amplitudes.

We now consider a particular class of ratio maps generated from "shell models." The latter can be viewed as the poor man's Navier–Stokes equations: instead of the whole velocity field, one retains only a discrete set of velocity amplitudes u_n, the dynamics of which is governed by a set of coupled differential equations of the form

$$\dot{u}_n = F_n(u_{n-s}, \dots, u_n, \dots, u_{n+s}) \tag{21}$$

where the F_n involve finitely many neighbors (in scale) of u_n. The various n's are referred to as "shells." Except for viscous and forcing terms, the F_n are chosen quadratic and satisfy energy conservation. We shall not here attempt any review of the considerable literature on shell models (see, e.g., refs. 10, 12, 26, and 27 and references therein). Our intention is to use a *static* form of shell models, i.e., we assume

$$F_n(u_{n-s}, \dots, u_n, \dots, u_{n+s}) = 0 \tag{22}$$

It is not our intention to discuss such thorny issues as: Are shell models "good" approximations to true turbulence? Can we learn something about the dynamics of shell models by studying the time-independent solutions?[4]

We just observe that static shell models immediately generate ratio maps of the form (20). Indeed, ignoring viscous and forcing terms, which

[4] Numerical simulations of the time-dependent GOY model and related models indicate that the solutions are "most of the time" static, with occasional violent time-dependent events.[28] Why this is so is not yet understood, but it gives added motivation to study the statics of such models.

are not relevant in the inertial range, and assuming that F_n is a homogeneous polynomial of degree two in the u_n, we find that $q_n = u_n/u_{n-1}$ satisfies a recursion relation of the form (20). An example will make this clear. One popular model is the Gledzer–Ohkitani–Yamada (GOY) model,[11,12] which, in its complete form (with viscosity, forcing, and time dependence), reads

$$\dot{u}_n^* + \nu k_n^2 u_n^* + f_n = F_n \equiv -ik_n(u_{n+1}u_{n+2} - \tfrac{1}{4}u_{n+1}u_{n-1} - \tfrac{1}{8}u_{n-2}u_{n-1}) \tag{23}$$

Here, ν is the viscosity, f_n is the forcing, and $k_n = l_n^{-1}$ is the shell wavenumber. The inviscid, unforced, and static GOY model gives

$$u_{n+1}u_{n+2} - \tfrac{1}{4}u_{n+1}u_{n-1} - \tfrac{1}{8}u_{n-2}u_{n-1} = 0 \tag{24}$$

Hence, the recursion relation for successive ratios is

$$q_n = \frac{1}{q_{n-1}q_{n-2}}\left(\frac{1}{4} + \frac{1}{8}\frac{1}{q_{n-1}q_{n-2}q_{n-3}}\right) \tag{25}$$

It turns out that the ratio map generated by the GOY model is quite trivial. Indeed, from (25) it follows that the product $z_n = q_n q_{n-1} q_{n-2}$ satisfies a first-order recurrence relation which has a single stable fixed point, $z_n = z_* = 2^{-1}$. Hence, there is no chaos, and K41 scaling is obtained. To obtain chaotic variations (in the shell index), we need to have more terms in F_n. One simple way is to perturb the GOY model by putting an admixture of another popular shell model, the Desnyansky–Novikov (DN) model.[10] In this way we generate the following ratio map:

$$\begin{gathered} q_n = f(q_{n-1}, q_{n-2}, q_{n-3}) \\ f(x, y, z) = \frac{1}{xy}\left\{\left(\frac{1}{4} + \frac{1}{8}\frac{1}{xyz}\right) + \gamma\left[\frac{1}{xy} - 2y + \delta\left(\frac{1}{x} - 2xy\right)\right]\right\} \end{gathered} \tag{26}$$

Here, δ is the so-called ratio of backward to forward cascade amplitudes in the DN model and γ is the admixture parameter, which in subsequent numerical computations will typically be taken small (about 10^{-2}). The hybrid ratio map (26), which will be referred to as GOY-DN in the sequel, has still a K41 fixed point $q_n = q_* = 2^{-1/3}$, but it is easy to find a region in the phase space of the parameters γ and δ where the K41 fixed point is unstable; for example, $\gamma > 0$, $\forall\delta$. Further information about the behavior of (26) requires numerical simulations.

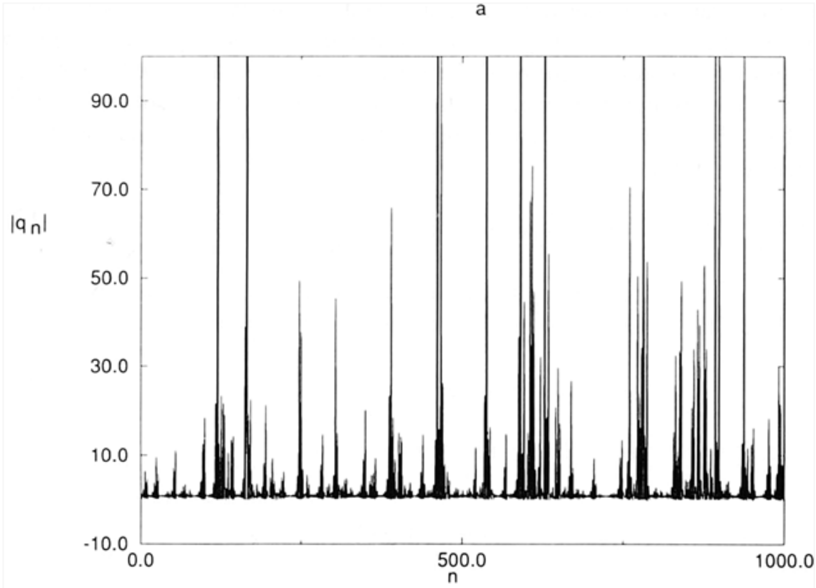

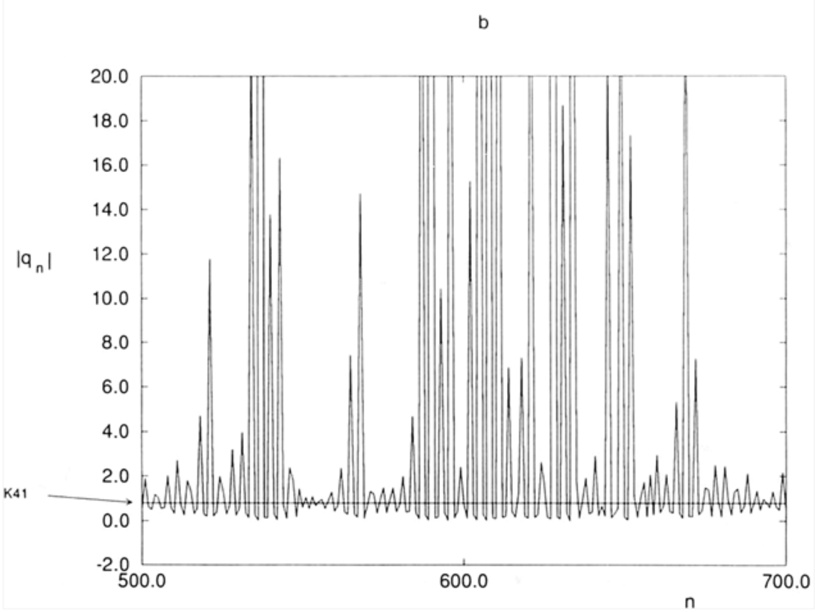

Fig. 2. (a) A typical solution of the difference equation (26). (b) A magnification of a portion of part (a). The horizontal solid line corresponds to the Kolmogorov fixed point.

4. NUMERICAL RESULTS

We found numerically that the GOY-DN map defined by (26) develops chaotic behavior for a sizable set of values of the control parameters γ and δ. Most of the numerical simulations reported hereafter were done with $\gamma = 0.01$ and $\delta = 4$. However, the qualitative feature of the results appears to be very stable against changes in the parameters, as long as the dynamics is chaotic.

Figure 2a shows a typical orbit of the map (26). The initial condition is obtained by adding a very small random perturbation (r.m.s. value about 10^{-5}) to the K41 fixed-point value. The orbit looks chaotic and also displays strong intermittent fluctuations. Its largest Lyapunov exponent is found to be about 0.22. The Kolmogorov fixed point, although it ceases to be stable as soon as $\gamma > 0$, still plays an important role in the dynamics. Figure 2b shows an enlargement of Fig. 2a, revealing that the orbit mostly oscillates close to the K41 fixed point, occasionally going on wild excursions. We mention that in the *unperturbed* GOY map, the K41 fixed point is neutrally stable: two eigenvalues of the derivatives matrix, calculated at the fixed point, have modulus one. Of course, the fixed point becomes completely unstable as soon as $\gamma > 0$.

We now turn to the structure functions (16), evaluated by averaging along the orbit with several million points. Figure 3 shows the structure

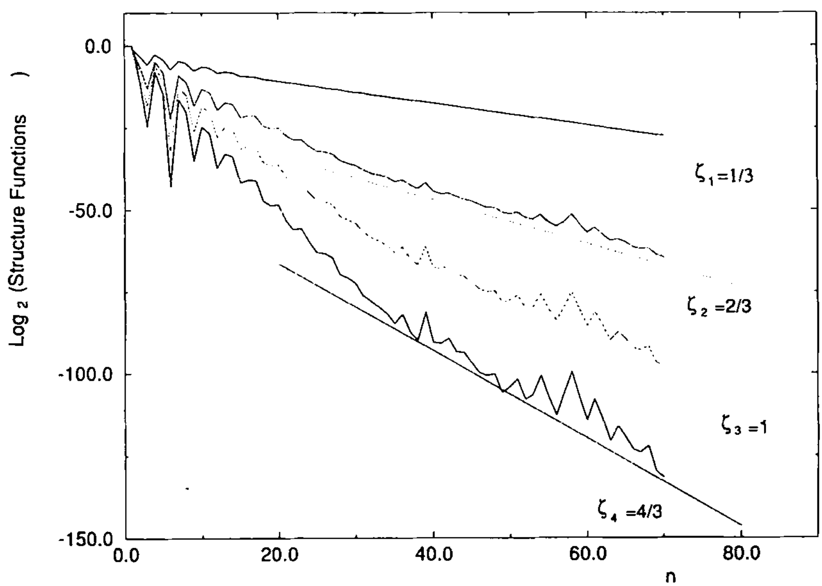

Fig. 3. Logarithmic plot of the structure functions $S_n^{(p)}$ as a function of n, for $p = 1, 2, 3, 4$. The solid lines correspond to the Kolmogorov 1941 scaling.

functions for p from 1 to 4. They are seen to follow power laws (in k_n) at large n. Except for some residual chaotic noise, the exponents are exactly given by their K41 value: $\zeta(p) = p/3$. Here, a word of warning is required. In numerical simulations of the full time-dependent shell models, it is not practical to have more than, say, 30 shells, since time steps decrease exponentially with n. Had we used such a low value of n for estimating exponents of structure functions, we would have predicted erroneous values, which would be misread as "multifractal" corrections to K41. We do not want here to open the Pandora's box of whether the multifractal corrections detected in the time-dependent simulations of shell models[26,27] are or are not finite-shell artefacts (similar questions can be asked for finite-Reynolds-number turbulence data).

The presence of exact K41 scaling suggests that the GOY-DN model has no large deviations. This can be checked directly by studying the probability density function (p.d.f.) $\pi(n, \Sigma)$ of the normalized sums of logarithms:

$$\Sigma(n) = \frac{1}{n} \sum_{k=1}^{n} \log_2 |q_k| \tag{27}$$

which plays in the deterministic case the role of (8) in the random case.

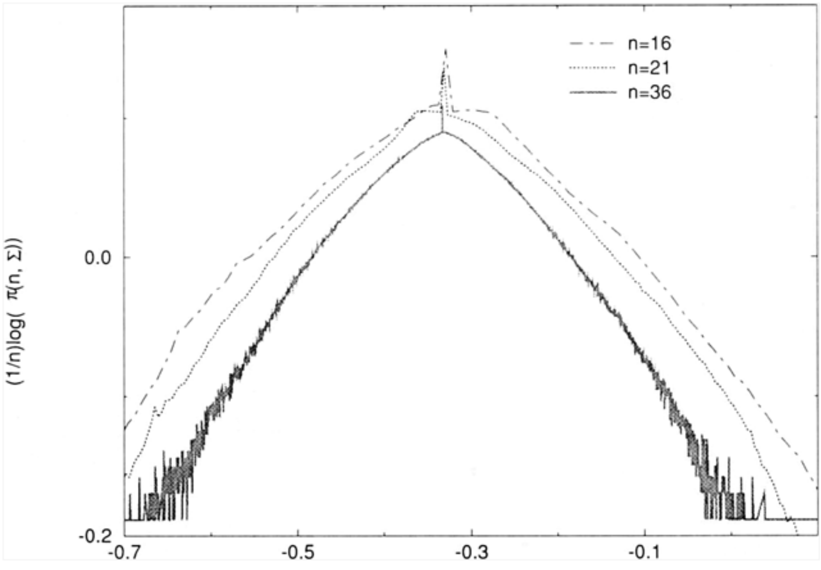

Fig. 4. Logarithm of the probability density function (p.d.f.) of $\Sigma(n)$, divided by n, for $n = 16$, 21, and 36. Notice that the peak at the Kolmogorov value $\Sigma(n) = -1/3$ becomes more pronounced as n increases.

Figure 4 shows the logarithm of the p.d.f. divided by n, $(1/n) \log(\pi(n, \Sigma))$, for three values of n. Note that as n grows, the curves become increasingly peaked at the K41 value $-1/3$. In the case of usual large deviations the p.d.f. $\pi(n, \Sigma)$ should decrease exponentially with n at fixed Σ, implying the various curves should settle down to a limiting curve. Our results suggest that $\pi(n, \Sigma)$ decreases faster then exponentially with n. [Possibly as $\exp(-n^{\omega})$, with $1 < \omega < 2$; finding the precise functional form would require considerably more numerical work.] Anyway, our results lead us to conjecture the absence of large deviations of the usual type. A possible interpretation of this phenomenon is presented in the next section.

5. NEUTRALLY UNSTABLE AND SPORADIC MAPS

We present a very simple example of a class of maps which displays chaos and no large deviations. Let us define

$$f_z(x) = \mathrm{Frac}(x^z + x): \quad [0, 1] \to [0, 1], \qquad z \geqslant 2 \tag{28}$$

The deterministic maps are chaotic, piecewise expanding, and have a neutral (or indifferent) fixed point at the origin. These maps are "sporadic," in the following sense[31]: The growth of infinitesimal errors is controlled by a stretched exponential with exponent less than one. Hence, the Lyapunov exponent is zero, although the maps certainly deserve to be called "chaotic." The derivative of any of these maps is equal to one at the origin and is strictly larger than one at all other points where it is well defined. This leads to some unusual ergodic properties, for example, the nonintegrability of the invariant measure, the density of which has a power-law singularity near the origin.[29-31] The reason is that once the orbit gets very close to the neutral fixed point, the time to escape from it is inversely proportional to a power of the distance from the fixed point. As a consequence, most usual ergodic averages such as (27) will be dominated by the contribution from the fixed point, so that there are no large deviations.

As for the absence of large deviations in the GOY-DN map (26), we are led to speculate that something similar happens: the presence of a neutrally unstable fixed point (or, more likely, a neutrally unstable periodic orbit) dominates the large-n asymptotics of structure functions.

Let us finally make two remarks. First, the positivity of the largest Lyapunov exponent in the GOY-DN map (26) is not inconsistent, as one would think at first, with the kind of behavior displayed by the maps (28) which have zero Lyapunov exponent. To illustrate this, consider the direct product of two one-dimensional maps: the first is any map chosen in the class (28) and the second is the piecewise linear map $g(y) = \mathrm{Frac}(2y)$ from

[0, 1] to itself. The product has as its largest Lyapunov exponent log 2. Nevertheless, for the observable $h(x, y) = xy$, ergodic averages of the logarithm of this function are still dominated by the contribution from $x = 0$, as if the multiplier y was absent. Second, let us mention that for the maps (28) it is possible to give an estimate of the average fraction of time during which the dynamics is chaotic.[31] This average goes to zero as a power law of the number of iterations n (e.g., as $\log n/n$, when $z = 2$). If the analogy between the sporadic maps and the GOY-DN model is correct, this suggests a possible interpretation of the rather strong corrections to K41 scaling at *finite n*, which eventually disappear at large n.

ACKNOWLEDGMENTS

The authors would like to thank V. Oseledets for discussions on the fast dynamo problems and G. Paladin for discussions on sporadicity and shell models. Very constructive remarks from the referees are also acknowledged. L.B. was supported by a Henri Poincaré fellowship (Centre National de la Recherche Scientifique and Conseil Général des Alpes Maritimes). M.B. was supported by the French Ministry of Higher Education.

REFERENCES

1. A. N. Kolmogorov, *Dokl. Akad. Nauk SSSR* **30**:301 (1941).
2. A. M. Obukhov, *J. Fluid. Mech.* **13**:77 (1962).
3. C. Meneveau and K. R. Sreenivasan, *J. Fluid Mech.* **224**:429 (1991).
4. E. Aurell, U. Frisch, J. Lutsko, and M. Vergassola, *J. Fluid Mech.* **238**:467 (1992).
5. F. Anselmet, Y. Gagne, E. J. Hopfinger, and R. A. Antonia, *J. Fluid Mech.* **140**:63 (1984).
6. C. Meneveau and K. R. Sreenivasan, *Nucl. Phys. B [Proc. Suppl.]* **2**:49 (1987).
7. A. Vincent and M. Meneguzzi, *J. Fluid Mech.* **225**:1 (1991).
8. G. Parisi and U. Frisch, in *Turbulence and Predictability in Geophysical Fluid Dynamics*, M. Ghil, R. Benzi, and G. Parisi, eds. (North-Holland, Amsterdam, 1985), p. 84.
9. R. Benzi, G. Paladin, G. Parisi, and A. Vulpiani, *J. Phys. A* **17**:3521 (1984).
10. V. N. Desnyansky and E. A. Novikov, *Izv. Akad. Nauk SSSR Fiz. Atmos. Okeana* **10**:127 (1974).
11. E. B. Gledzer, *Sov. Phys. Dokl.* **18**:216 (1973).
12. M. Yamada and K. Ohkitani, *J. Phys. Soc. Jpn.* **56**:4210 (1987).
13. E. A. Novikov and R. W. Stewart, *Izv. Akad Nauk SSSR Ser. Geoffiz.* **3**:408 (1964).
14. A. Yaglom, *Dokl. Akad. Nauk SSSR* **166**:49 (1966).
15. B. B. Mandelbrot, *J. Fluid Mech.* **62**:331 (1974).
16. Y. Oono, *Progr. Theor. Phys. Suppl.* **99**:165 (1989).
17. P. Collet and F. Koukiou, *Commun. Math. Phys.* **47**:329 (1992).
18. H. Cramér, Colloque consacré à la théorie des probabilités, *Actualités Sci. Industrielles* **736**:5 (1938).
19. S. R. S. Varadhan, *Large Deviations and Applications* (SIAM, 1984).
20. R. S. Ellis, *Entropy and Equilibrium States in Classical Mechanics* (Springer, 1985).
21. B. B. Mandelbrot, *Proc. R. Soc. Lond. A* **434**:79 (1991).

22. M. Blank, *Uspekhi Matem. Nauk* **44**:3 (1989).
23. V. I. Arnold, Ya. B. Zeldovich, A. A. Ruzmaikin, and D. D. Sokoloff, *Sov. Phys. JETP* **54**:1083 (1981).
24. E. Aurell and A. D. Gilbert, Fast dynamo and determinants of singular integral operators, *Geophys. Astrophys. Fluid Dyn.*, in press (1993).
25. V. Oseledets, Fast dynamo problem for a smooth map on two-torus, to be published.
26. M. H. Jensen, G. Paladin, and A. Vulpiani, *Phys. Rev. A* **43**:798 (1991).
27. D. Pisarenko, L. Biferale, D. Courvoisier, U. Frisch, and M. Vergassola, *Phys. Fluids A* **5**:2533 (1993).
28. E. Lévêque, Private communication (1993).
29. M. Blank, *Chaos* **1**:347 (1991).
30. P. Collet and P. Ferrero, *Ann. Inst. H. Poincaré* **52**:283 (1990).
31. P. Gaspard and X.-J. Wang, *Proc. Natl. Acad. Sci. USA* **85**:4591 (1988).